Mechanics & Industry **18**, 114 (2017)

DOI: 10.1051/meca/2015073
www.mechanics-industry.org

Mechanics & Industry

Burr height monitoring while drilling CFRP/titanium/aluminium stacks

Xavier Rimpault[1,a], Jean-François Chatelain[2], Jolanta Ewa Klemberg-Sapieha[3] and Marek Balazinski[1]

[1] Department of Mechanical Engineering, École Polytechnique de Montréal, Montréal, QC, Canada
[2] Department of Mechanical Engineering, École de Technologie Supérieure, Montréal, QC, Canada
[3] Department of Engineering Physics, École Polytechnique de Montréal, Montréal, QC, Canada

Received 30 October 2014, Accepted 28 September 2015

Abstract – In the aerospace industry, deburring operations are often difficult to achieve and can be very costly. Hence, burrs generated during the machining should be studied. In this research, the drilling operations were performed and analysed for a stack composed of carbon fibre reinforced polymer (CFRP), titanium and aluminium alloys, using three cutting feeds and three cutting speeds for each material. A monitoring method is presented to predict the burr heights in the titanium and aluminium layers. The cutting force signals obtained during the drilling of the CFRP layer were analysed using the regularization fractal analysis, resulting in an estimation of the fractal dimension. This fractal analysis was optimized in order to monitor the clearance tool wear and the burr heights. The burr heights, measured at the outlet of the titanium and aluminium alloys, were observed in terms of the thrust force, the torque, the hole diameter and circularity, and the clearance tool wear. This fractal analysis technique can be implemented for an on-line control to predict the generated burr heights in the metallic layers while drilling the previous CFRP layer.

Key words: Stack drilling / burr height / fractal analysis

1 Introduction

The use of carbon fibre reinforced polymer (CFRP) has been increasing over the past decades in the aircraft structures, notably due to its high strength/weight ratio. During airplane assembly, CFRP panels are used alongside with metallic parts, e.g. made of aluminium or titanium alloys. In the aerospace industry, to assemble and fasten those parts together, traditional drilling and mechanical bolting operations are usually conducted. The drilling process can be operated on different types of stacks, such as: CFRP/titanium, CFRP/aluminium, aluminium/CFRP/titanium, etc. Bolting is used in order to assemble the parts and also to easily dismantle them for maintenance and repair purposes. Nevertheless, to increase the hole precision, all layers of the stack should be machined at once. Therefore, one-shot drilling is preferred [1].

On the other hand, the one-shot drilling process yields additional problems. Tönsheff et al. [2] found that when drilling of sandwiched materials, various problems may occur, such as dissimilar diameter, intense tool wear, heat damage, intra- and inter-laminate delamination, erosion, etc.

Moreover, the hole quality, such as the hole surface roughness and the hole straightness to the generating line, greatly impacts the efficiency of the bolting joints. It is therefore desirable to machine holes with tight hole straightness tolerances. However, drilling operation is more challenging to control, particularly due to the different machining characteristics of the layers within the stack [3]. In this study, the diameter of the hole is measured at different hieghts along the hole depth.

Burr formation is a critical factor occurring during the drilling of metallic parts. After machining operations, parts are deburred which cost can account for up to 30% of the total cost of the components [4]. However, in the aerospace industry, before stacking and drilling of the parts together, a shim resin is usually applied between each layer. That complicates the observation of one part only and the measurement of its burr heights [5].

In this paper, two main aspects were studied. The first one is the burr heights measured at the outlet of the metallic layers. The second one is the monitoring and

[a] Corresponding author:
xavier.rimpault@polymtl.ca

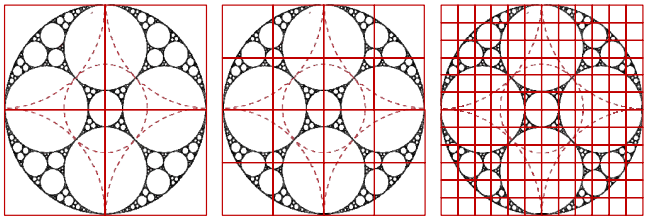

Fig. 1. Box counting example for a five circle inversion fractal.

diagnosis of the burr heights and the tool wear thanks to the fractal analysis of the cutting force signals from the CFRP machining. The generated burrs remain a challenge in the industry and needs to be evaluated through the scope of various elements such as the tool wear, the cutting parameters and the cutting forces. The fractal analysis of the cutting force signals allows monitoring the burr height generated and so keeping required inside burr height tolerance.

2 Fractal analysis

The term "fractal" was first introduced by Mandelbrot [6] to describe the "roughness" or singularities or length of the coastline of Britain. Depending on the scale of the observation of a coastline, the length may vary. The traditional geometrical approach is ineffective to provide an accurate measurement of the coastline length. A fractal is an object or a set which owns a self-affine or self-similar pattern or singularity [7]. Fractals can be defined by their fractal dimension. This parameter may be estimated through few fractal analyses. One of the simplest and probably the most commonly used is the capacity fractal analysis, also called the box counting fractal analysis. This technique is illustrated in Figure 1. The object is observed through a mesh with a box size of ε. For each mesh size, boxes that contain a part of the object are numbered giving the minimal number of boxes number N_ε required to cover the object.

Then, the capacity dimension can be expressed as follows:

$$D_C = -\lim_{\varepsilon \to 0} \frac{\ln(N_\varepsilon)}{\ln \varepsilon} \quad (1)$$

For the example from Figure 1, the calculated capacity dimension D_C is close to 1.328, the fractal dimension of this object.

Fractal analysis is used to provide a measure of the irregularity or "roughness" of a signal from a dynamic system. The health information of a machine or its subset parts can be extracted from the fractal analysis of their vibration signals [8,9].

Few fractal analysis methods can be found in the literature. One of them, the regularization analysis, was used for signals analysis in order to describe the irregularities in non-linear dynamical systems [8]. This method is used in this study to show its possibilities to analyse the cutting force signals. One of the main reasons of choosing this method is its robustness [10]. Feng et al. [6] used it for processing the accelerometer signal to assess the gear damage.

Besides, contrary to isotropic and homogenous materials such as metal alloys, CFRP is made of two different components – carbon fibres which are very hard to machine and epoxy resin which has a high machinability index. During the machining of CFRP, the carbon fibres are fractured due to the mechanical load of the tool applied on the fibre.

The fracture of the carbon fibres causes an additional noise on the cutting forces signals comparing to the signals obtained during the machining of the homogenous metallic materials. This noise may depend on the wear state of the tool, the nose radius, the cutting parameters, etc.

Usually, this noise is not taken into account in the analysis of the cutting forces. However, it may give additional information relative to the machining such as the tool condition, the quality of the surface generated and the hole surface condition. With the increase of the tool wear or the change of the cutting parameters, the noise – or "roughness" – on the signal might change. Indeed, to fracture the fibres with a worn tool, the mechanical load applied may need to be higher. In this case, the use of fractal analysis could give a possibility of monitoring the tool condition by analysing the noise from the cutting force signals.

3 Workpiece materials

3.1 CFRP

Besides problems occurring due to the stacking of different materials, various issues may appear from the drilling process: fibre-resin delamination which could appear at the inlet or outlet of the hole, burnt composite, pulled and uncut fibres, etc. [11–13].

Due to the high sensibility of the epoxy resin to the heat, the temperature generated during the drilling can locally burn the resin. Due to the low conductivity of the epoxy resin, the temperature is difficult to ease. Thus, during dry drilling, the machining generates higher temperatures than with coolant use.

Due to the abrasiveness and hardness of the carbon fibres, abrasion is the main wear mechanism affecting the tool [14]. Tsao et al. [15] shown that the tool condition has an impact on the tool wear: an increased tool wear leads to more delamination. They found that delamination can also be influenced by the feed rate and the drill diameter.

3.2 Titanium alloy

Titanium alloys are widely used in the aerospace industry thanks to their superior properties e.g. a high strength/weight ratio, a low density, a high fatigue and a high corrosion resistance. But, titanium alloys are also known to be difficult-to-machine materials [16].

Their low thermal conductivity causes high temperatures generated in the primary cutting zone during machining That results in an intense and rapid tool wear [17,18].

In addition to the severe tool wear, the surface integrity and the quality of the holes drilled are influenced mostly by the high temperature in the cutting zone. This impact may be observed through the surface roughness parameters, the burr height, the hole diameter, as well as the changes in the microstructure near the surface of the walls of the holes [19].

Because of the generated heat caused by the drilling of the titanium layer, the experiments were conducted using peck drilling to, consequently, reduce this heat [4,20,21].

3.3 Aluminium alloy

Contrary to titanium alloys, aluminium alloys have excellent machinability properties. Although the aluminium machinability index is relatively high, problems occur when drilling such alloys. One of the main problems is the adhesion of cut material on the tool cutting edges. This causes a tool wear increase and consequently to a low surface quality. On one hand, increasing the cutting speed can reduce this adhesion effect. But, on the other hand, the cutting speed increase raises as well the temperature in the cutting zone [22,23].

Commonly used in the aerospace industry, the aluminium grade selected is one of the 7000 aluminium series. This grade was chosen for its good characteristics, such as high machinability index, high strength and heat treatment capacity. The drawback of this grade is its low resistance to corrosion [24,25].

4 Experimental set-up

The upper layer of the composite/metal stack tested was a CFRP laminate manufactured with an autoclave-cured 24-ply CFRP laminate using the pre-impregnated ply technology. This CFRP was prepared with lay-up continuous unidirectional fibre layers with 0° , 90° and ± 45° orientations, with a total thickness of 3.3 mm and a volume fibre fraction of 64%. The titanium layer was a Ti-6Al-4V, with a thickness of 2.0 mm. The aluminium layer was comprised of one 3.5 mm thick 7000 series aluminium grade.

The machining experiments were carried out using the high speed machining centre Huron® K2X10. This 3-axis computerised numerical control (CNC) machine allows a maximum spindle speed of 28 000 RPM at 40 kW. For health and safety purposes, a dust extraction system was mounted onto the machine.

Figure 2 depicts the components of the workpiece used for the experiments. In industrial application, shim resin is applied between each layer of the stack. However, to allow the measurement and the analysis of the burr heights, shim was not applied and a thermoreactive paper® was placed instead. Due to the high heat generated during the machining of the titanium layer, the thermoreactive paper side was placed towards the titanium layer. This 0.05 mm thick paper allows a temperature range detection at the interface of two materials to see if the temperature generated at the interfaces was not too high to affect the materials of the stack. The reactive range of this colour-reacted paper detects temperatures between 90 °C and 150 °C. Above the upper limit, the paper becomes darker and darker until it combusts.

Fig. 2. Stack material specifications.

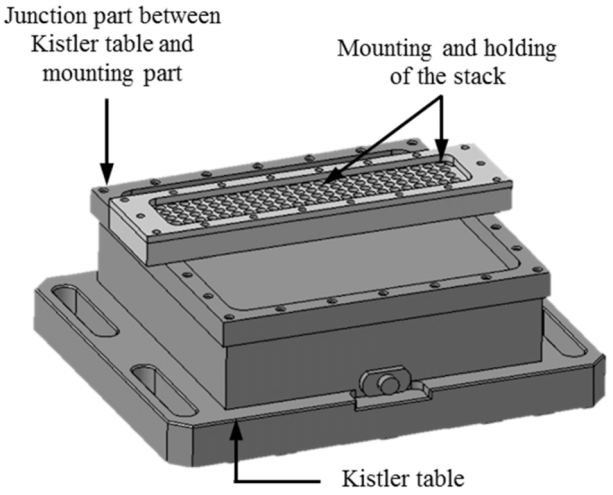

Fig. 3. Experimental set-up of the fixture of the workpiece, mounted over the Kistler force measurement table and a junction part.

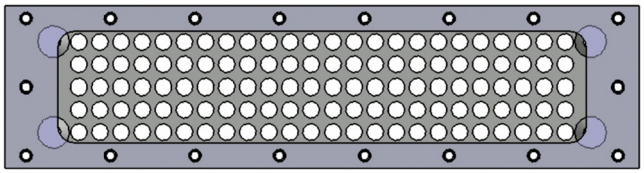

Fig. 4. Top view of the holding table and frame of the stack.

The experimental set-up is shown in Figure 3. A sponge filled with coolant was placed close to the working area allowing to slightly lubricate the tool tip during the drilling of the metallic layers.

Figure 4 shows the mounting that allows the drilling of 120 holes, with a maximum diameter of 6 mm in an 80 mm × 300 mm workpiece.

The torque and thrust force were measured for each drilling using a 9255B Kistler® piezoelectric dynamometer table. The signals obtained were transmitted through an amplifier. Then, the signals were digitalised using an A/D converter with a 24 MHz frequency rate and recorded with a data acquisition set.

Table 1. Conducted plans of experiments for the twist drills.

Tool #	Number of holes drilled	Experiments
1	118	2 Taguchi + 1 Full
2	64	1 Taguchi + 1 Strategy
3	56	1 Full + 1 Strategy

5 Methodology

5.1 Design of experiments

The aim of the conducted experiments was to improve the stability of the process, as well as the hole quality during the drilling of the multimaterial stack composed of CFRP, titanium and aluminium alloys. Therefore, burr heights were inspected in the outlets of the metallic layers. Different cutting parameters, as well as different drilling strategies, were applied during those experiments. The heights of pecks during peck drilling, the feed variations while cutting, and the heights of cutting parameter changes (from one material cutting parameters to another) were the chosen parameters for the drilling strategy. Nevertheless, due to a minor impact of the selected drilling strategies, only the cutting parameters variations versus the burr heights were presented. Three cutting feed and three cutting speed levels were selected for each type of material within the stack. The design of experiments, which was divided into two parts, included a $L_{27}(3^6)$ Taguchi plan of experiment and a full plan of the couple feed-speed for each of the three materials.

Only the cutting parameters were selected as experiment variables for these two plans of experiments. Each design of experiments was performed three times and the order of the drillings was randomized for each repetition.

Three twist drills, with a common geometry and coating, were used to perform two series of 120 holes. During the experiments, the drills were put in contact with a sponge filled with coolant before each change of cutting parameters. The use of these diamond-coated tools is listed in Table 1.

The levels of the cutting parameters are presented as normalised values using the central selected point as the cutting parameter reference.

5.2 Analyses performed

Analyses of variance (ANOVA) were performed for the thrust force, the torque burr height, the hole diameter and the circularity, allowing an identification of their impact and the quantification of the different cutting parameters.

The fractal dimensions of the CFRP cutting force signals were calculated using the regularization fractal analysis to evaluate the complexity of the signal. The regularization fractal analysis was chosen for its relative robustness [8,10].

Regularization dimension is obtained after convolutions of the signal s with different Gaussian kernel g_a with a width of a. Then, the convolution product s_a can be expressed:

$$s_a = s * g_a \tag{2}$$

The Gaussian kernel g_a used in our calculation was the first derivative of the 1-D Gaussian function with a width of a.

The hypothesis is that s_a has a finite length called l_a, for the size of a [10,26]. The regularization dimension D_R is then obtained with:

$$D_R = 1 - \lim_{a \to 0} \frac{\ln l_a}{\ln a} \tag{3}$$

The limit, in the Equation (3), is usually estimated as the slope value when a values are close to 0 and when the coefficient of determination R-squared of the linear regression of a part of the curve is close to 1.

The thrust force signals obtained during the machining of the CFRP layer were analysed with this regularization technique giving the fractal dimensions. The relation between the computed fractal dimensions and the number of holes previously drilled was observed, as well the relations between the calculated fractal dimensions and the tool wear VB_B max and between the calculated fractal dimensions and the burr height ratio in the titanium and in the aluminium outlets.

Although the fractal dimension was computed on the torque and the thrust force signals acquired during the machining of the CFRP, titanium and aluminium, only the results of the thrust force fractal dimension during the CFRP machining are presented in this article.

5.3 Measurements

The on-line measurements of cutting forces – thrust force and torque – were performed. The average values, calculated from the cutting force signals, were compared to the burr height ratio. As well as for the cutting parameter values, the results of the burr heights are presented as normalized, in percentage. The burr height ratio corresponds to the measured burr height over the maximum burr height obtained for the layer.

A digital probe indicator was used to measure the hole burr heights at the outlet of the titanium and aluminium layers. For each hole, the burr height value was assessed as an average of three measurements.

Both clearance faces of the twist drills were inspected every five drillings using the digital optical microscope VHX-600+500F Keyence®. The tool wear VB_B max was estimated using the digital images captured with the microscope. The tool wear VB_B max presented in this article is expressed as the average of the tool wear estimated on both drill faces.

The hole dimensions were measured using the Mitutoyo Bright Strato coordinate measuring machine (CMM) in order to check the hole straightness to the generating line. The diameter and circularity were measured for each hole, and at the same depths from their references A, B

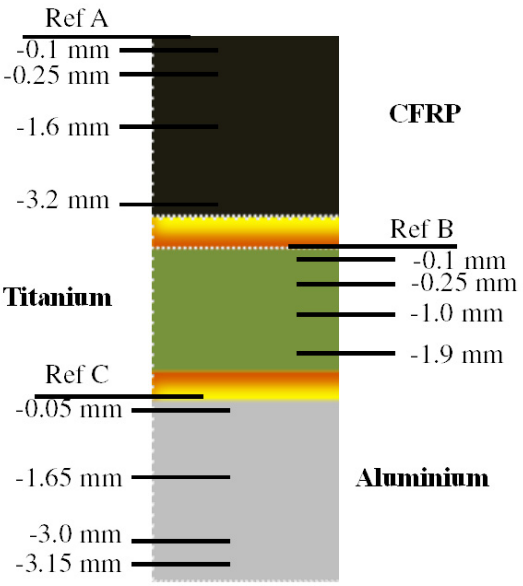

Fig. 5. Depths for the measurements of hole diameter and circularity (the references are at the top of each layer in the stack).

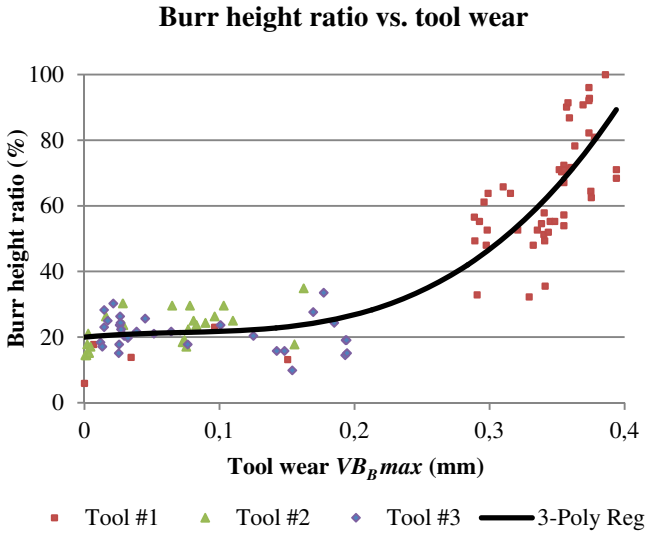

Fig. 6. Titanium burr height ratio versus the tool wear VB_B max.

and C, for CFRP, titanium and aluminium, respectively, as depicted in Figure 5.

The presented thrust force and torque values are the averages of the signal obtained during one peck when the drill cutting edges are fully engaged in a same material. The final thrust force and torque values are estimated by the average of all the pecks.

6 Results and discussion

6.1 Burr height analysis

6.1.1 Titanium burr height analysis

The tool wear of identical tools can differ from the same cutting conditions after a certain number of drilled holes. This is why the burr height versus the tool wear was preferred to the burr height versus the number of drilled holes. The evolution of the measured titanium burr heights versus the measured clearance tool wear VB_B max is shown in Figure 6. A regression was calculated using a third-order polynomial function showing the dependency between the burr height ratio and the tool wear.

Moreover, although the experiments were conducted on the stack of materials where there was no clearance at the titanium layer outlet, no limit seems to be reached by the burr heights. Nonetheless, the burr heights measured should instinctively tend to a maximum value for a high tool wear, due to the presence of the aluminium layer at the outlet side of the titanium layer. Two possible reasons can be taken into consideration. Firstly, the limit of the tool wear may not have been reached in our tests. In this case, further experiments might show a maximum or at least a reduction in the burr height increase versus the tool wear. The second reason may be that the mechanical characteristic differs for the titanium and aluminium alloys. Under the pressure applied from the tool during machining, the titanium burr is pushed onto the aluminium layer. Due to the lower hardness of the aluminium comparatively to the titanium, the aluminium part is locally deformed by the titanium burr.

Table 2. Means of the titanium burr height ratios for each couple of feed and speed corresponding to the titanium layer.

Feed/Speed levels	Titanium speed 70%	Titanium speed 100%	Titanium speed 130%
Titanium feed 60%	51.3	48.5	50.6
Titanium feed 100%	42.9	43.9	42.2
Titanium feed 140%	36.6	40.4	26.8

The results of the titanium burr heights versus the thrust force and the torque are presented in Figures 7 and 8, respectively. The presented results were obtained from the titanium machining with the same cutting conditions in the titanium layer, which cutting parameters where selected at the central point of the titanium cutting speed and feed levels. The R-squared coefficient, calculated from the linear regression, is lower for the torque due to a higher dispersion, which equals 0.77 for Figure 7 and 0.5 for Figure 8.

The means of the burr height ratio measured for each set of cutting parameters are shown in Table 2. According to the results, the cutting speed in the titanium layer does not affect significantly the burr height as opposed to the cutting feed. The higher the feed is, the lower the burr heights are.

The relative standard deviation of the burr height was calculated using the measurement results of the holes drilled with the same cutting conditions with a tool wear lower than 0.20 mm, giving the result of 5.5%.

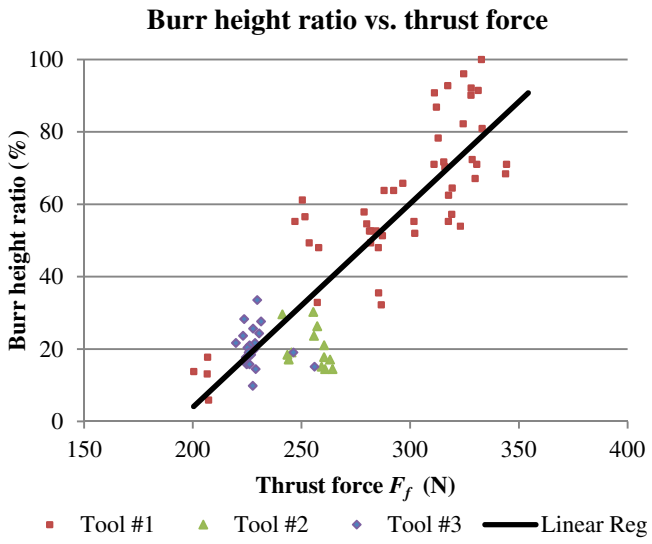

Fig. 7. Titanium burr height ratio versus the thrust force under same cutting parameters corresponding to the central point of the variation parameters for titanium.

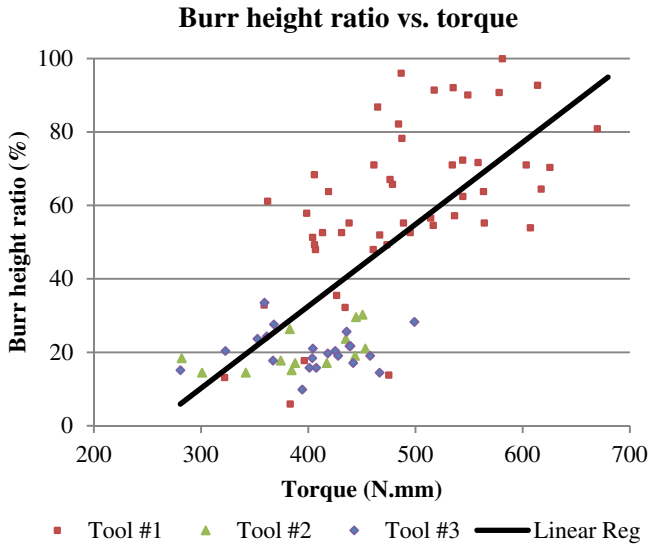

Fig. 8. Titanium burr height ratio versus the torque under same cutting parameters corresponding to the central point of the variation parameters for titanium.

On the thermoreactive paper, a dark halo around the hole was observed for each hole. The radial value of the halo was measured on the thermoreactive paper placed between the titanium and aluminium layers where the titanium burrs are investigated. The measured radial values of the halo were within the range between 0.02 mm and 0.05 mm. No other colour could be identified around this halo. Thus, the temperature gradient at the outer limits of the halo was high.

6.1.2 Aluminium burr height analysis

Firstly, the observations at the outlet of the holes on the aluminium layer presented no attachment onto the exit surface such as ring or drill cap. This statement was valid for all the cutting feed or speed levels and for all the cutting strategy selected.

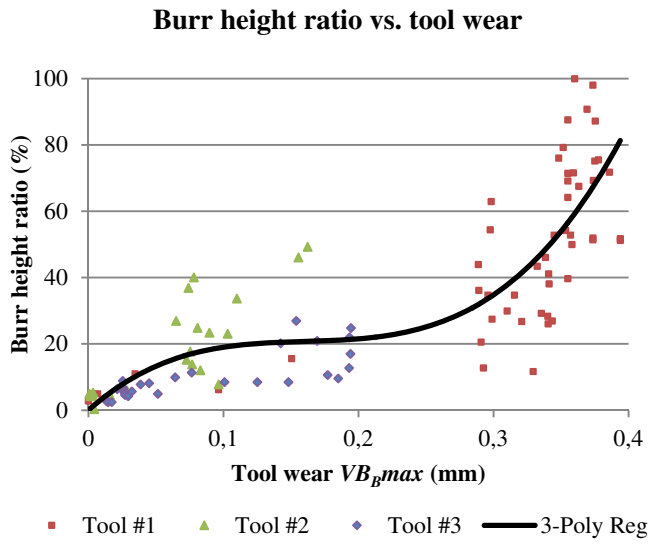

Fig. 9. Aluminium burr height ratio versus the tool wear VB_B max.

The evolution of the measured aluminium burr height versus the tool wear VB_B max is depicted in Figure 9. A regression was calculated using a third-order polynomial function showing the dependency between the burr height ratio and the tool wear.

Figure 10 shows the measured aluminium burr height versus the thrust force. The dependency between the burr height and the thrust force is illustrated by the calculated exponential regression function drawn in Figure 10. The R-squared coefficient calculated from the exponential regression equals 0.54. Although a correlation can be observed between the burr height and thrust force, no significant correlation can be detected between the torque and the aluminium burr heights. Dispersion of the results is relatively high and the correlation coefficient calculated was close to zero.

Table 3 shows the means of the burr height ratios measured for each set of aluminium cutting parameters. According to these results, for high cutting speed, the aluminium burr heights remains steady whatever the feed is. However, for low and central cutting speed levels, higher burr heights are generated for higher cutting feed levels.

The relative standard deviation calculated for the aluminium burr height was computed using the measurement results of the holes drilled with the same cutting conditions with a tool wear inferior to 0.20 mm, giving the result of approximately 10%.

6.2 Fractal analysis of cutting forces

The observation of the cutting force signals during drilling the CFRP, titanium and aluminium suggested performing fractal analysis on those signals. Figures 11 and 12 show an example of the measured thrust force

Table 3. Means of the aluminium burr height ratios for each couple of feed and speed corresponding to the aluminium layer.

Feed/Speed levels	Aluminium speed 60%	Aluminium speed 100%	Aluminium speed 140%
Aluminium feed 75%	29.2	31.0	33.7
Aluminium feed 100%	34.6	35.7	32.2
Aluminium feed 125%	40.5	42.0	32.9

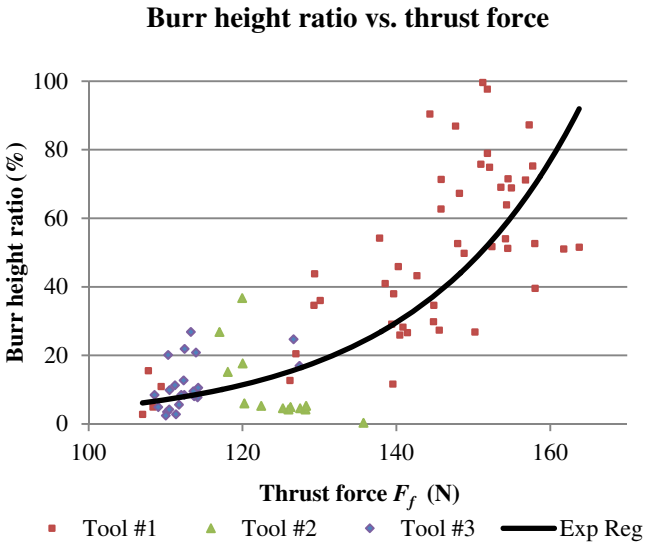

Fig. 10. Aluminium burr height ratio versus the thrust force under same cutting parameters corresponding to the central point of the variation parameters for titanium.

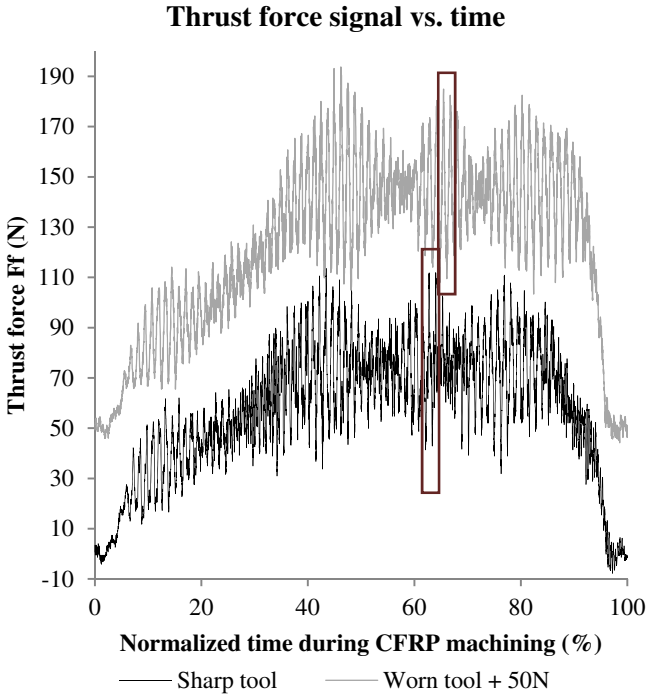

Fig. 11. Measured thrust force signals for sharp and worn tools during CFRP machining.

signals during the machining of CFRP, obtained with a sharp tool and a worn tool.

The signal acquired during the whole CFRP machining, shown in Figure 11, highlights the more erratic character of the sharp tool comparing to the worn one. This observation is confirmed with the graph presented in Figure 12 which is a magnification of the frames from Figure 11. The worn tool signal over a period seems to be close to a periodical function whereas the signal is more irregular.

As mentioned above, the regularization fractal analysis was processed on the signals of the cutting force. In the preliminary study, it was performed for the thrust force signals obtained with one tool at different tool wear levels under the same cutting conditions. Figure 13 shows the graph $\ln l_a$ (length of the convolution product estimated for the size a) versus $\ln a$, for one tool while drilling the hole numbers 1, 17, 34, 55, 82 and 115. In order to estimate the slope value and so, the fractal dimension, the least square (LS) method was used. However, it is crucial to determine the range where the slope value is calculated. According to the fractal dimension definition, this range is selected where the slope derivative remains stable and for the lowest values of a. Nevertheless, we found that the obtained results from such a range show very low impact towards the number of holes drilled or the tool wear. Depending on the scale of observation, the noise from the dynamometer or the CNC machine prevails on the signal

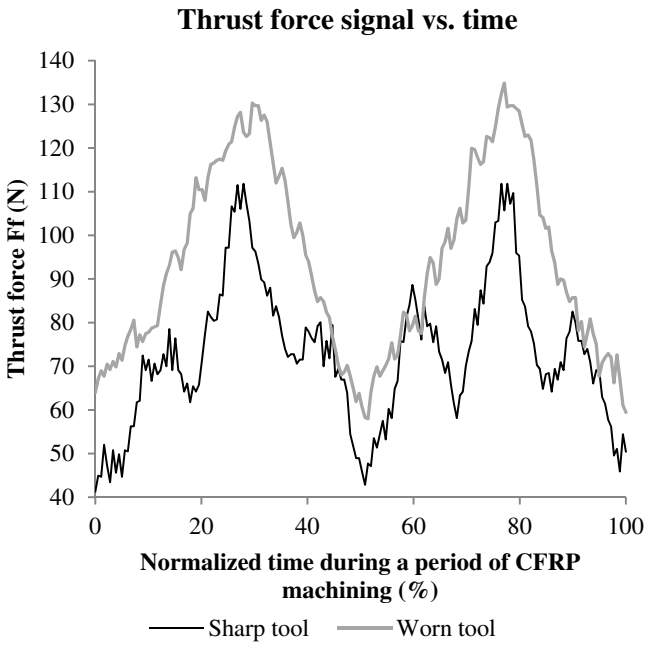

Fig. 12. Measured thrust force signals for sharp and worn tools over a period during CFRP drilling (magnification of the frames from Fig. 11).

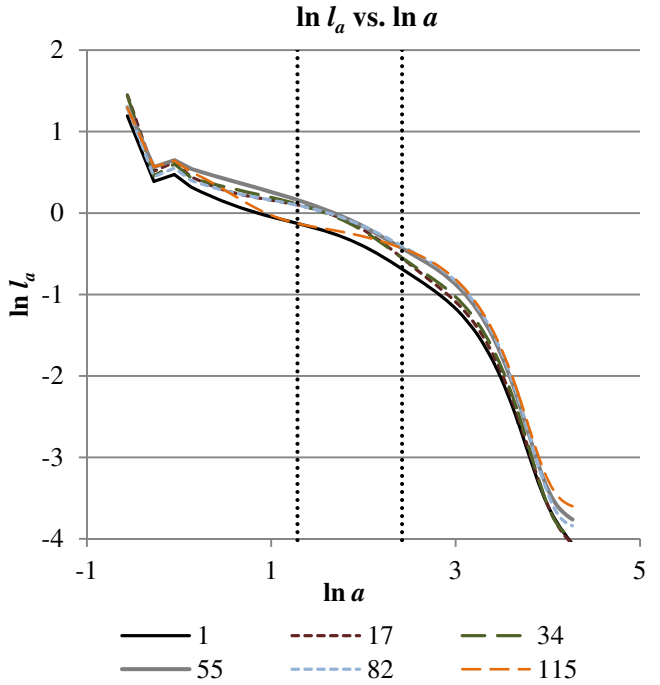

Fig. 13. Graphs ln l_a (length of the convolution product estimated for the size a) versus ln a computed from the thrust force signals obtained during the CFRP machining using one tool after drilling the holes 1, 17, 34, 55, 82 and 115.

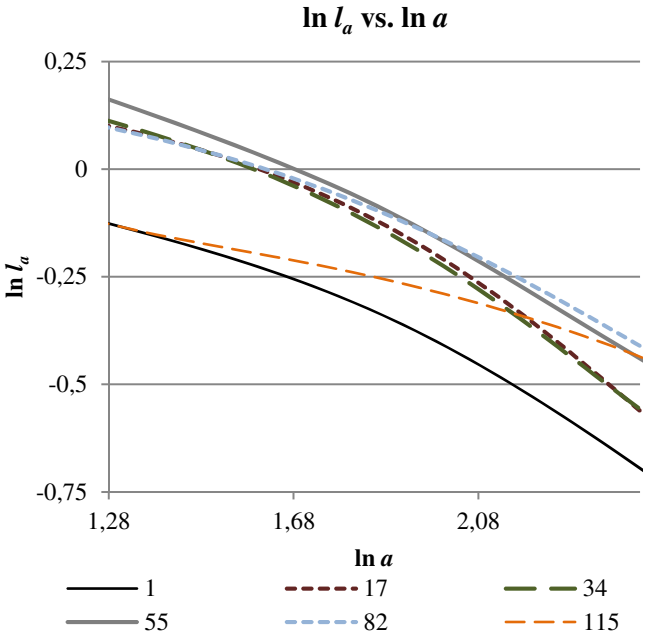

Fig. 14. Graphs ln l_a (length of the convolution product estimated for the size a) versus ln a from the thrust force signals obtained from the CFRP machining using one tool after drilling the holes 1, 17, 34, 55, 82 and 115 (magnification of the area between the vertical lines from Fig. 13).

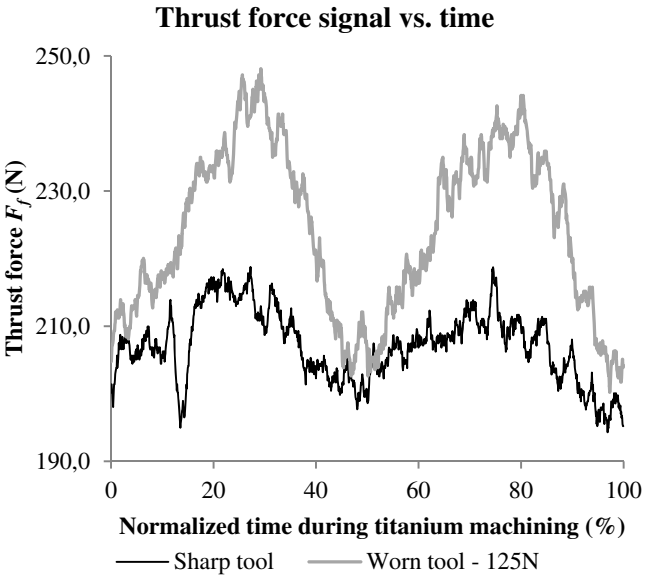

Fig. 15. Measured thrust force signals for sharp and worn tools over a period during titanium machining.

of the cutting forces. This is why the range determination needs to be re-established.

From preliminary analyses, the best fit for the upper limit of this range was found for the sampling points acquired during one third of the tool rotation period. The lower limit was selected for a fixed sampling length, which does not depend on the cutting speed. No relevant feed rate impact was found over those two limits. This range selection was used for the following fractal dimension estimations. The selected range between those upper and lower limits is represented by dot lines in Figure 13. The graph presented in Figure 14 corresponds to the magnification of the graph area within the selected range in Figure 13.

For each hole, the regularization fractal analysis was performed on the thrust force and on the torque signals from the CFRP machining. Though, only the results computed from the thrust force show less dispersion and are presented.

This analysis was similarly realized on the torque and on the thrust force signals obtained during the titanium and aluminium machining. From this investigation, the computed fractal dimensions show an even higher dispersion. However, the use of the fractal analysis on the cutting force signals in these homogeneous materials, such as employed aluminium and titanium alloys, may not be relevant. Even if the shape of the cutting force signals is more jagged with a worn tool, the difference is not as visible as for the signals from the CFRP machining. Figure 15 depicts the thrust force signals for a sharp tool and a worn tool over one tool rotation period. Admittedly, the amplitudes of both periodical curves are different, but they share, relatively, similar curvature and similar noise.

After adapting the regularization fractal analysis to our case, the repeatability of this analysis needs to be check to evaluate the results. Fractal dimension was calculated for different sampling lengths of a single thrust force signal. Each relative standard deviation was computed from one hundred fractal dimensions D_R

Table 4. Means of the calculated force signal fractal dimensions D_R for each couple of feed and speed levels corresponding to the CFRP layer.

Feed/Speed levels	CFRP Speed 60%	CFRP Speed 100%	CFRP Speed 140%
CFRP Feed 70%	1.66	1.59	1.50
CFRP Feed 100%	1.65	1.53	1.46
CFRP Feed 130%	1.57	1.56	1.45

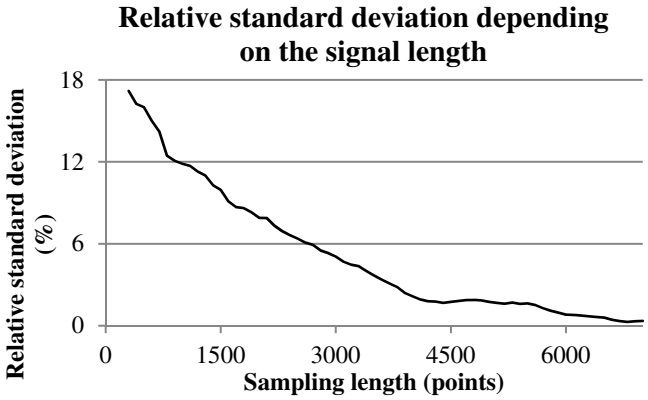

Fig. 16. Relative standard deviations of fractal dimensions D_R, calculated for different sampling lengths.

calculated from signal sections. The relative standard deviations were calculated using different sampling lengths, which is presented in Figure 16.

The relative standard deviation is around 17% for short signal lengths (around 300 points). For a treated signal of 4000 points and more, the relative standard deviation drops under 2%. All the signals analysed from the CFRP machining had a wider length than 4000 points.

Table 4 shows the means of the fractal dimensions D_R, computed on the thrust force signals during the CFRP drilling for each hole. The means were calculated for each level of the CFRP cutting parameters (feed and speed). Those mean values point a maximum of 15% variation and need to be taken into account for further considerations. Figure 17 depicts the calculated dimensions for cutting speed and feed at 100%. For each signal, three slope values were estimated using the LS method and the minimum (Min) and maximum (Max) limits by consecutives eliminations.

All the results of the calculated fractal dimension versus the tool wear VB_B max are presented in Figure 18. A third degree polynomial regression was drawn with a 0.52 R-squared value. The fractal dimension remains relatively constant until it drastically drops for a higher tool wear.

Figures 19 and 20 depict the fractal dimensions versus the titanium burr height ratio and the aluminium burr height ratio, respectively. For all the results, regardless the cutting parameters of any layer, a linear regression was drawn as an approximation of the results with a R-squared value of 0.45 for both, titanium and aluminium, burr heights. Regarding the results of the aluminium burrs for one tool used with same cutting parameters selected, the R-squared score jumps to 0.65 and

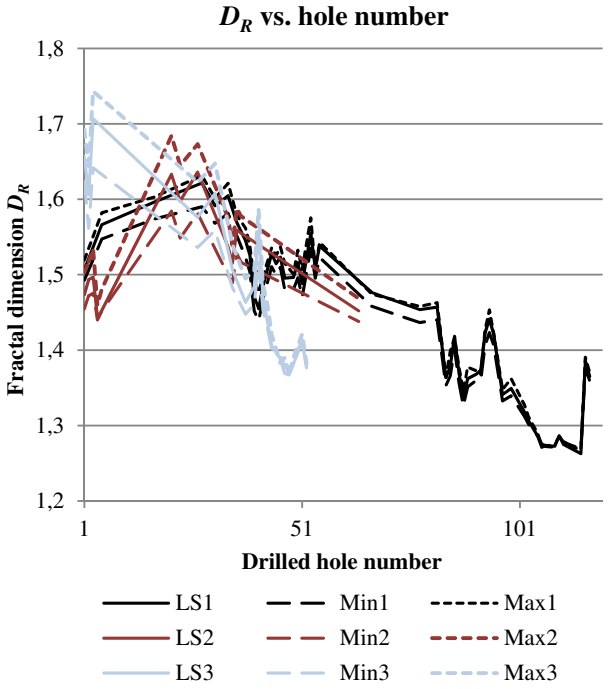

Fig. 17. Fractal dimension D_R versus the number of hole drilled for 100% CFRP cutting speed and feed levels (LS 1–3: fractal dimension D_R estimated with least square method for tools 1–3, Min: minimum limit of fractal dimension D_R, Max: maximum limit of fractal dimension D_R).

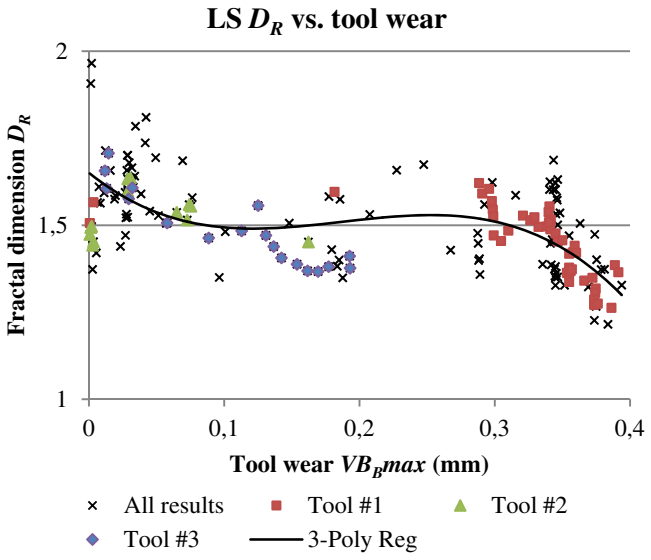

Fig. 18. Fractal dimensions D_R using least square (LS) method versus the tool wear VB_B max.

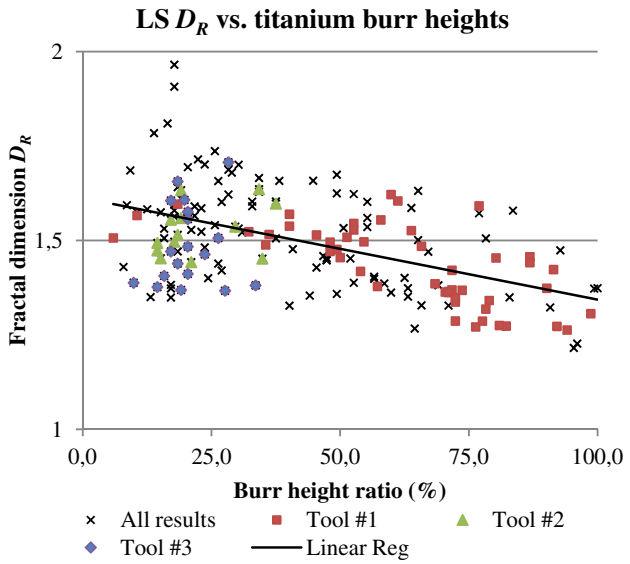

Fig. 19. Fractal dimensions D_R using least square (LS) method versus titanium burr height ratio.

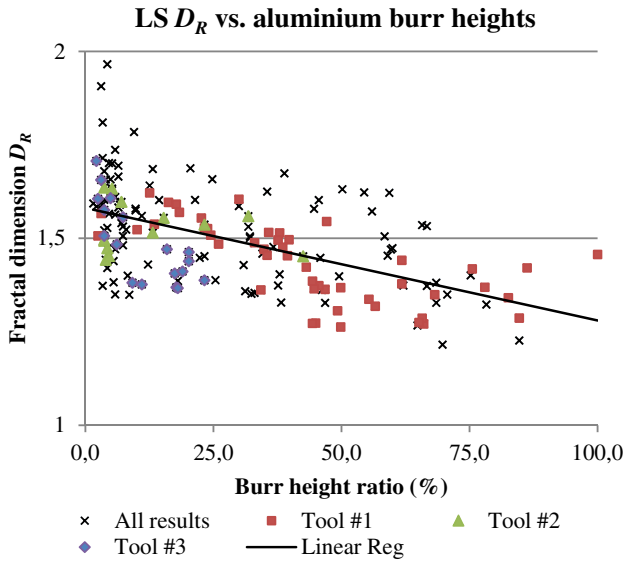

Fig. 20. Fractal dimensions D_R using least square (LS) method versus aluminium burr height ratio.

0.84 with a two and three degree polynomial regression, respectively.

In addition to the tool wear or cutting forces in titanium and aluminium layers, fractal dimension D_R calculated from the thrust force signals during the CFRP machining can be another feature to monitor the burr generation. It may also be possible to evaluate the tool wear. The advantage of this method results in the prediction of the burr heights in the titanium and aluminium outlets before the tool drills these layers. This allows preventing off-tolerance burr heights without altering the production time.

7 Conclusion

A method to monitor the burr heights in a multimaterial stack was developed based on the regularization fractal analysis. In the industry, a deburring process may not be performed following the drilling of a multimaterial stack, the burr heights need to be monitored. The thrust force signals acquired during the drilling of the CFRP layer were analysed using an adaptation of the regularization analysis, giving the fractal dimension. This fractal dimension allows to monitor and to estimate the burr heights in the metallic layers of the stack composed of CFRP, titanium and aluminium. Using the cutting forces obtained from a dynamometer table, the burr heights can be estimated when the tool is drilling the CFRP layer and before it reaches the titanium and aluminium layers. Hence, this technique allows preventing to generate hole burr heights outside tolerance requirements and improving production efficiency. Even if the use of a dynamometer table remains complicated to integrate in some industry processes, this analysis and monitoring technique may be implemented e.g. for signals from AE sensors placed onto the CNC machine relatively close to the spindle.

To feature this monitoring technique, multimaterial stack drilling experiments were conducted using diamond-coated twist drills. The burr heights versus factors such as speed and feed levels, tool wear, thrust force, torque, diameter and circularity were studied. The results show that the titanium burr heights can be reduced using a higher feed. For titanium burrs, the process can be observed thanks to the torque average while drilling the titanium layer and, for more accuracy, with the thrust force average. The tool wear is also an effective way to check the burr height. The aluminium burrs can be reduced by increasing the cutting speed or by decreasing the feed. The aluminium burrs can be monitored as well with the thrust force average while drilling the aluminium layer, and also with the tool wear.

Acknowledgements. The authors wish to thank the Consortium for Research and Innovation in Aerospace in Québec (CRIAQ) and its partners, the Natural Sciences and Engineering Research Council of Canada (NSERC), Mitacs, Bombardier Aerospace, Avior Integrated Products, Delastek and AVR&R Aerospatiale, for their financial support. The regularization fractal dimensions were computed based on the program code of the FracLab software developed by INRIA France.

References

[1] E. Brinksmeier, R. Janssen, Drilling of Multi-Layer Composite Materials consisting of Carbon Fiber Reinforced Plastics (CFRP), Titanium and Aluminum Alloys, CIRP Annals - Manufact. Technol. 51 (2002) 87–90

[2] J.L. Cantero, M.M. Tardio, J.A. Canteli, M. Marcos, M.H. Miguelez, Dry drilling of alloy Ti-6Al-4V, Int. J. Machine Tools Manufact. 45 (2005) 1246–1255

[3] A.I.H. Comittee, Machining, ASM Handbook, ASM International, 1992, p. 929

[4] A.I.H. Comittee, Properties and Selection : Nonferrrous Alloys and Special-Purpose Materials, ASM Handbook, ASM International, 1992, p. 3470
[5] D.A. Dornfeld, J.S. Kim, H. Dechow, J. Hewson, L.J. Chen, Drilling Burr Formation in Titanium Alloy, Ti-6AI-4V, CIRP Ann. – Manuf. Technol. 48 (1999) 73–76
[6] Z. Feng, M.J. Zuo, F. Chu, Application of regularization dimension to gear damage assessment, Mech. Syst. Signal Process. 24 (2010) 1081–1098
[7] P. Guegan, F. Lemaitre, J. Hamann, Contribution à l'usinage des matériaux composites, La Construction Navale en Composites, edited by I. Brest, Paris, France, 1992, p. 11
[8] W. König, C. Wulf, P. Graß, H. Willerscheid, Machining of Fibre Reinforced Plastics, CIRP Ann. – Manuf. Technol. 34 (1985) 537–548
[9] J. Lévy Véhel, P. Legrand, Signal and image processing with Fraclab, in: C.A.F.i.N. Proceedings of Fractal04 Eighth International Multidisciplinary Conference, Vancouver, Canada, 2004
[10] G. List, M. Nouari, D. Géhin, S. Gomez, J.P. Manaud, Y. Le Petitcorps, F. Girot, Wear behaviour of cemented carbide tools in dry machining of aluminium alloy, Wear 259 (2005) 1177–1189
[11] B. Mandelbrot, Les objets fractals: Forme, hasard et dimension, Flammarion, France, 1975
[12] J. Mathew, N. Ramakrishnan, N.K. Naik, Investigations into the effect of geometry of a trepanning tool on thrust and torque during drilling of GFRP composites, J. Mater. Process. Technol. 91 (1999) 1–11
[13] A. Molinari, C. Musquar, G. Sutter, Adiabatic shear banding in high speed machining of Ti-6Al-4V: experiments and modeling, Int. J. Plasticity 18 (2002) 443–459
[14] M. Nouari, G. List, F. Girot, D. Géhin, Effect of machining parameters and coating on wear mechanisms in dry drilling of aluminium alloys, Int. J. Machine Tools Manufact. 45 (2005) 1436–1442
[15] E. Persson, I. Eriksson, L. Zackrisson, Effects of hole machining defects on strength and fatigue life of composite laminates, Compos. Part A: Appl. Sci. Manufact. 28 (1997) 141–151
[16] I.J. Polmear, Light Alloys – Metallurgy of the Light Metals, Halsted Press, 1996
[17] M. Ramulu, T. Branson, D. Kim, A study on the drilling of composite and titanium stacks, Compos. Struct. 54 (2001) 67–77
[18] F. Roueff, J. Lévy Véhel, A Regularization Approach to Fractional Dimension Estimation, Fractals 98, edited by M.M. Novak, World Scientific, 1998
[19] B. Sapoval, Universalités et fractales, Science, Flammarion, France, 1997
[20] I.S. Shyha, S.L. Soo, D.K. Aspinwall, S. Bradley, R. Perry, P. Harden, S. Dawson, Hole quality assessment following drilling of metallic-composite stacks, Int. J. Machine Tools Manufact. 51 (2011) 569–578
[21] D.A. Stephenson, J.S. Agapiou, Metal cutting theory and practice, CRC press, 2005
[22] H.K. Tönsheff, T. Friemuth, M. Groppe, A solution for an economical machining of bore holes in composite materials (CFK, aluminum), in: Proceedings of 3rd International Conference on Metal Cutting and High Speed Machining, Metz, France, 2001
[23] C.C. Tsao, H. Hocheng, Effect of tool wear on delamination in drilling composite materials, Int. J. Mech. Sci. 49 (2007) 983–988
[24] J. Yang, Y. Zhang, Y. Zhu, Intelligent fault diagnosis of rolling element bearing based on SVMs and fractal dimension, Mech. Syst. Signal Process. 21 (2007) 2012–2024
[25] X. Yang, C. Richard Liu, Machining titanium and its alloys, Machin. Sci. Technol. 3 (1999) 107–139
[26] P.F. Zhang, N.J. Churi, Z.J. Pei, C. Treadwell, Mechanical drilling processes for titanium alloys: a literature review, Machin. Sci. Technol. 12 (2008) 417–444